1986MNRAS.223..763M

Mon. Not. R. astr. Soc. (1986) **223,** 763–786

The light from Population III stars

Jonathan C. McDowell* *Institute of Astronomy, Madingley Road, Cambridge CB3 0HA*

Accepted 1986 June 24. Received 1986 June 24; in original form 1985 October 14

Summary. It has been suggested that the first generation of stars may have been Very Massive Objects (VMOs) which existed for a brief period and left a large fraction of the mass of the Universe in black hole remnants which now provide the dynamical 'dark matter'. If the radiation from these stars was not thermalized to distort the microwave background, it would be present today as a separate cosmological isotropic background radiation at some waveband from the infrared to the ultraviolet, depending on the redshift of the sources and whether any absorption and re-emission of the radiation by dust occurred. We calculate the expected spectrum from such a population of stars under a variety of assumptions about their environment and the intergalactic medium. By comparing the expected background with observed upper limits with such radiation fields, upper limits to the density provided by such stars can be obtained. Using the present observational data, the simplest model indicates that such stars cannot close the Universe if they formed at a redshift of less than 40, and cannot even provide missing mass equal to one-tenth of the critical density (as required for the mass in galactic haloes) if they existed at a redshift of less than 30. In all models, such stars must have formed at redshifts greater than 5 if they form the dark matter in haloes.

1 Introduction

In this paper we use the term 'Population III' to refer to a first generation of stars which may be pregalactic or may be present in young galaxies. We investigate some consequences of the suggestion developed by various workers that these stars may have been very massive (over $100\,M_\odot$) hydrogen–helium objects containing effectively no metals. This scenario has recently been described by Carr, Bond & Arnett (1984); this paper represents an extension of the work reported there. In particular, we attempt to constrain the possibility that these first-generation stars left black hole remnants which would now make up the dark matter that is implied by measurements of the dynamics of galaxies and clusters of galaxies (White & Rees 1978). If there

*Present address: Nuffield Radio Astronomy Laboratories, Jodrell Bank, Macclesfield, Cheshire SK11 9DL.

© Royal Astronomical Society • Provided by the NASA Astrophysics Data System

1986MNRAS.223..763M

really is non-baryonic dark matter it is likely to be very difficult to prove its existence, and it is therefore important to rule out alternative explanations.

Our constraints are based on the light that would have been generated by such a first generation of stars. Although they would be dark matter now, they would have been very luminous in their stellar phase. The light that they generated will now contribute to the diffuse extragalactic background light. Possible sources of extinction in the Universe – dust, neutral hydrogen, electron scattering – will not alter the intensity of the radiation but just redistribute it in frequency. Clearly, at very high redshifts the $1+z$ loss in photon energy will make the sources undetectable; we attempt to find, for each model we consider, the redshift beyond which the background would be below the observational limits. This type of calculation was performed by Peebles & Partridge (1967) for the expected background from protogalaxies; one of their models included a Population III generation of sufficient density to make the first metals. Such a population has quite a small mass density and produces a fairly small intensity of background light; in contrast, our models attempting to make up the dark matter must efficiently suppress enrichment of the metals (by asserting that the nucleosynthesis products are contained within the remnants). Thorstensen & Partridge (1975) also considered the background light constraint, but only in the context of a closure density of the objects.

We characterize the Population III objects by the approximate redshift at which they form and the cosmological mass density they make up in units of the closure density. The use of redshift as our time parameter means that the background light limits derived below are essentially independent of the specific Friedmann cosmological model except for a simple dependence on the Hubble constant H_0. We shall assume that the nuclear-burning time-scale of the stars is small compared with the cosmological expansion time-scale. In the redshift regime of a few ($z \approx \Omega^{-1}$) to a hundred we can adopt the approximate time–redshift relation

$$t = \tfrac{2}{3} H_0^{-1} \Omega_0^{-1/2} z^{-3/2} \tag{1.1}$$

which enables us to estimate the relative size of various time-scales and the expansion time-scale, and in the first part of the paper we use this approximation to study the Very Massive Object (VMO) environment. (This approximation is not used in deriving the background light limits themselves, which are independent of Ω_0 except in the models with intergalactic dust where the limits depend weakly on Ω_0 via the total optical path length for a given redshift. For these dusty models we have adopted for the results presented here a total density parameter of unity, but other runs with $\Omega_0 = 0.1$ give similar curves.) We shall normalize the Hubble constant by setting $h_{50} = H_0/(50\,\mathrm{km\,s^{-1}\,Mpc^{-1}})$, so that $\tfrac{2}{3} H_0^{-1} = 1.3 \times 10^{10}/h_{50}\,\mathrm{yr}$. Now let ϱ_c be the closure density ($\varrho_c = 4.7 \times 10^{-27} h_{50}^{-2}\,\mathrm{kg\,m^{-3}}$). We define dimensionless mass densities Ω of stars, gas, etc. in units of this quantity ($\Omega_* = \varrho_*/\varrho_c$, $\Omega_g = \varrho_g/\varrho_c$), giving the contribution to the total cosmological density parameter from each of these sorts of matter.

2 Properties of Very Massive Objects

Carr *et al.* (1984) conclude that stars with normal masses present in large quantities in the Population III era would enrich the interstellar medium with metals to a degree incompatible with the existence of low-metallicity Population II stars. They also discuss other reasons why VMOs are preferred candidates for Population III objects. Bond, Arnett & Carr (1984, hereafter BAC) study the properties of Population III VMOs and derive analytical approximations to their structure. These massive stars are quite well approximated by a constant-entropy Eddington model; BAC use a point-source model to develop an improved analytical approximation to the stellar structure. Population III VMOs which develop a central oxygen core mass of more than

© Royal Astronomical Society • Provided by the NASA Astrophysics Data System

1986MNRAS.223..763M

$100\,M_\odot$ collapse to black holes, while smaller ones explode. The initial mass of a star which has this critical final mass depends on the unknown details of mass loss but is at least $200\,M_\odot$. We adopt as a reference model a $100\,M_\odot$ model with a hydrogen abundance of 0.75 and an internal metal abundance of $Z=10^{-9}$. Such a metal abundance would be generated by a zero-metal star early in its evolution. This BAC model has a temperature of $T=1.0\times10^5$ K and a main-sequence

Table 1. Observational limits.

Wavelength (μm)	Effective bandwidth	$\log\nu$	$\log\omega_\nu$	Reference
650	625–665	11.66	−4.3	1
590	570–610	11.71	−4.3	1
500	490–510	11.78	−4.3	1
500	350–3000	11.78	−4.0	2
425	415–435	11.85	−4.3	1
200	150–400	12.18	−4.36	3
100	80–230	12.48	−4.52	4
60	40–80	12.70	−4.46	4
25	19–30	13.08	−3.40	4
12	8–15	13.40	−3.35	4
4.7	4.4–5.0	13.81	−3.92	5
4.2	3.8–4.5	13.85	−4.17	5
3.8	3.4–4.1	13.90	−4.10	5
2.4	2.35–2.45	14.10	−3.84	6
2.2	2.0–2.4	14.13	−4.19	5
1.6	1.45–1.75	14.27	−4.14	5
Wavelength (Å)	Effective bandwidth	$\log\nu$	$\log\omega_\nu$	Reference
5115	5070–5160	14.77	−5.59	7
4400	3950–4850	14.83	−5.70	8
3100	2850–3350	14.99	−5.60	9
2200	2000–2400	15.13	−6.24	9
1790	1690–1890	15.22	−6.22	10
1690	1520–1860	15.25	−5.82	9
1680	1580–1780	15.25	−6.05	10
1550	1500–1650	15.29	−6.40	11
1450	1400–1500	15.32	−6.40	11
1350	1300–1400	15.35	−6.40	11
1250	1220–1500	15.38	−6.30	12

The parameter $\omega(\nu)$ is the energy density per logarithmic frequency interval in units of the critical density needed to close the Universe. The values are tabulated for $H=50\,\mathrm{km\,s^{-1}\,Mpc^{-1}}$.

[1] Woody & Richards (1981); balloon flight, Texas.
[2] Ceccarelli *et al.* (1984); dipole anisotropy limit on data of De Bernardis *et al.* (1984).
[3] De Bernardis *et al.* (1984); balloon flight, Sicily.
[4] Hauser *et al.* (1984); *IRAS* satellite, low Earth orbit.
[5] Matsumoto, Akiba & Murakami (1984); *Kappa-9M* rocket flight, Japan.
[6] Hoffmann & Lemke (1978); balloon flight, Texas.
[7] Dube *et al.* (1979); Kitt Peak, Arizona.
[8] Toller (1983); *Pioneer 10* space probe, beyond the asteroid belt.
[9] Maucherat-Joubart, Deharveng & Cruvellier (1980); *Aura* satellite low Earth orbit.
[10] Severniy & Zverezda (1983); *Prognoz-6* satellite, cis-lunar space.
[11] Feldman, Brune & Henry (1981); *Aries* rocket, White Sands, New Mexico.
[12] Weller (1983); *Solrad 11B* satellite, cis-lunar space.

© Royal Astronomical Society • Provided by the NASA Astrophysics Data System

1986MNRAS.223..763M

life of $t_{ms}=3.4\times10^6$ yr during which it converts a fraction $\varepsilon=0.0034$ of its rest mass to energy. The star emits $\dot{N}=1.05\times10^{50}$ ionizing photons per second. We parameterize the change in these properties with mass by the quantities

$$f_\varepsilon=\varepsilon/0.0034$$

$$f_T=T/10^5\,\mathrm{K}$$

$$f_t=t_{ms}/3.4\times10^6\,\mathrm{yr}$$

$$f_N=\dot{N}/1.05\times10^{50}\,M_2\,\mathrm{s}^{-1}. \quad (2.1)$$

These parameters are functions of the mass, which we write as $M=100\,M_2\,M_\odot$. These slowly varying functions are tabulated for a few values of M_2 in Table 1; they have been evaluated from the point-source model formulae in BAC. Although we are only interested in stars which turn into black holes, which means values of M_2 which may be substantially above unity, the fact that the f parameters are slowly varying means that the results are actually independent of M_2. For some of the numerical calculations presented in Section 7, models with a mass of 200 $M_\odot$ were actually used. However, the background radiation generated only depends on the luminosity ε, per unit mass, which is approximately constant. Note that the main-sequence time is shorter than the expansion time for $z<240\,\Omega^{-1/3}h_{50}^{-2/3}$, justifying the remarks in Section 1.

3 The background light limits

Attempted observations of the extragalactic background light have been made in almost every waveband. In this study we consider limits in the region from the far ultraviolet to the far infrared. The values of the energy density corresponding to the observations are listed in Table 2 as values of the parameter $\omega(\nu)$ defined by equation (6.2) (the energy density per unit logarithmic

Table 2. Values of the smallest redshift $z(\Omega_*)$, at which the model in question exceeds the observational limits.

(a) Models with no dust

	$H_0=50$			$H_0=100$		
	$\Omega_*=0.01$	$\Omega_*=0.1$	$\Omega_*=1$	$\Omega_*=0.01$	$\Omega_*=0.1$	$\Omega_*=1$
BB	13	29	40	23	36	180
	18	43	76	32	65	150
R	3.5	3.5	20	4.7	5.9	42

(b) Blackbody model with varying dust abundance

	$H_0=50$			$H_0=100$	
Ω_d	$\Omega_*=0.01$	$\Omega_*=0.1$	$\Omega_*=1$	$\Omega_*=0.01$	$\Omega_*=0.1$
0	13	29	40	23	36
10^{-6}	11	24	81	–	–
10^{-5}	7.5	11	76	3.5	25
10^{-4}	2.3	5.5	62	5.6	9.0

(c) Blackbody model with dust forming more recently

	$H_0=50$		
z_d	$\Omega_*=0.01$	$\Omega_*=0.1$	$\Omega_*=1$
3	2.4	18	32
5	2.3	5	46
10	2.3	5.3	65
100	2.3	5.5	62

© Royal Astronomical Society • Provided by the NASA Astrophysics Data System

1986MNRAS.223..763M

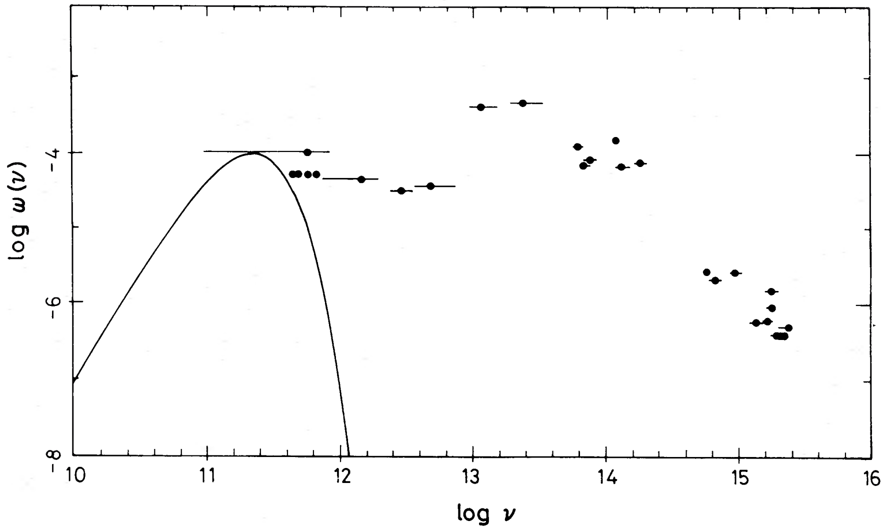

Figure 1. Extragalactic background light limits: observational limits in the present energy density of extragalactic background light. The data of Table 1 are plotted against logarithmic frequency. The horizontal bars represent the bandwidth of the observations. The microwave background is represented by the full curve.

frequency interval in units of the critical density) and are plotted in Fig. 1 together with a 3 K blackbody spectrum representing the microwave background. In both Table 2 and Fig. 1 we have taken $h_{50}=1$. The observations are in all cases treated as upper limits to the possible contribution from pregalactic stars; thus we do not need to evaluate other possible contributions to the background, nor do we try to 'explain' detected backgrounds.

In the far infrared, the limits are from dipole anisotropy measurements at wavelengths of several hundred microns (Ceccarelli *et al.* 1984) and the *IRAS* preliminary results on diffuse emission (Hauser *et al.* 1984). Rowan-Robinson (1986) argues that there is a residual unexplained roughly isotropic background with substantial energy density at 100 μm; his analysis requires detailed assumptions about the dust composition, and we shall take the *IRAS* measurement as an upper limit only. The results of Matsumoto *et al.* (1984), originally claimed as a detection of a near-infrared background, are now only claimed as an upper limit. The extrapolation of the *IRAS* results to lower wavelengths is not inconsistent with the Japanese data (J. Negroponte, personal communication). There are no data on background light in the red part of the visible spectrum; a weak limit could be placed by the zodiacal light brightness at the ecliptic pole but it does not set useful constraints. The optical limits are from Dube *et al.* (1979) and Toller (1983); Toller's observations were made from beyond the asteroid belt and should be free from most Solar System background light. Ultraviolet limits have been taken from a number of satellite experiments; these observations represent a positive detection of ultraviolet background light but it is not clear how much of it is extragalactic in origin. The result of Weller (1983) from a US Navy satellite sets a strong limit in the far ultraviolet.

For each spectral model, the expected flux for a given redshift of origin is calculated for each of the observational bands and the strongest limit for that redshift is selected. As discussed in Section 7, we illustrate our results as a series of curves showing limits to the possible mass density in VMOs as a function of redshift. This limit is expressed as a value of Ω_*. Since the black hole remnants of these stars could have accreted matter over the intervening period, we cannot exclude a higher density in the remnants. Carr (1979) sets limits on accreting black holes; our limits only apply to the amount of mass in the stars in the nuclear-burning phase. Limits on accretion radiation from individual remnants in our own Galaxy have been calculated by McDowell (1985).

© Royal Astronomical Society • Provided by the NASA Astrophysics Data System

1986MNRAS.223..763M

4 The opacity of the Very Massive Object environment

To understand the present form of any background radiation field due to VMOs we must investigate the extinction in the neighbourhood of the source and in the Universe as a whole. We shall argue that there is so much uncertainty in our knowledge of physical conditions at redshifts of more than 1 or 2 that the radiation could be either quite unaffected or completely altered. There are three main possible outcomes.

(a) The spectrum is unaltered.

(b) The spectrum is absorbed above the Lyman limit by neutral hydrogen and dominated by the resulting recombination line radiation. We shall consider a simple model for this by assuming that each ionizing photon is replaced by one Lyman α photon and then present limits from a more detailed calculation.

(c) The spectrum is absorbed by dust. The photons will then be scattered into the infrared. If the optical depth were large, the spectrum would be thermalized even at infrared wavelengths and could in principle be responsible for the cosmic microwave background. More probably, as we shall show, the radiation will be scattered only once and either distort the microwave background [this has been discussed previously (Layzer & Hively 1973; Rees 1978; Negroponte, Rowan-Robinson & Silk 1979)] or provide a separate far-infrared background (Bond, Carr & Hogan 1986).

First we shall study absorption of the star's light at the epoch of its production. The main sources of opacity will be dust and neutral hydrogen. The optical depth may be significant in any of a number of regions around the star – the star's own mass-loss atmosphere, the nebula within which it formed, the interstellar medium of any protogalaxy in which it might be embedded and the background Universe itself. To the extent that they can all be modelled as regions of constant density, all but the first of these sites can be treated in the same way. The mass-loss atmosphere is treated separately.

4.1 ABSORPTION LOCAL TO THE SOURCES

Consider a nebula of density profile $n(r)$ surrounding the star or a group of the stars. Let the number of hydrogen atoms in the cloud per star be $\beta Y_H M/m_H$, so that the ratio of the mass in the clouds to the mass in the stars is β and the hydrogen abundance is Y_H. Note that this fraction β may be large, but if the sources make up the dark matter it will be less than unity at a typical time in the Population III era unless the holes accrete most of their mass subsequently. For a given volume of gas we now determine the density that the nebula must have in order to absorb all the incoming radiation. As a simple approximation we consider a one-zone model with a single temperature and balance ionizations caused by the star with those recombinations which do not involve the production of ionizing photons. This is the 'on-the-spot' approximation in which ionizing photons produced in the cooling of the gas are reabsorbed immediately. If α_{eff} is the effective recombination rate (i.e. excluding re-ionizing recombinations),

$$\dot{N} = \int \alpha_{eff} n^2 \, dV. \tag{4.1}$$

We shall temporarily ignore re-ionizations caused free–free photons and $n \geq 2$ recombination continuum photons. α_{eff} is then simply the recombination coefficient to all levels excluding the ground state; $\alpha_{eff} = 3.7 \times 10^{-20} T_5^{-0.8}\,\mathrm{m^3\,s^{-1}}$ (Kaplan & Pikel'ner 1970) and depends on the nebular temperature $T = 10^5 T_5$ K. The intense stellar flux will maintain T_5 close to unity despite cooling due to hydrogen and helium, in contrast with the normal metallicity case where line cooling by oxygen and other metals would lower T_5 to 0.1 or so. If the nebula is very thin,

© Royal Astronomical Society • Provided by the NASA Astrophysics Data System

1986MNRAS.223..763M

Compton cooling by the microwave background photons may be an important effect, but we shall see that the nebula must be very dense to affect the outgoing radiation.

In addition the gas may contain dust; in the true first generation of stars there will of course be no dust, but in succeeding generations of stars there may be a small abundance. If the dust mass fraction is χ. The Lyman limit optical depth is

$$\tau_0=\sigma_0\chi\int n\,dr \tag{4.2}$$

where $\sigma_0\chi$ is the dust optical depth per unit hydrogen column (and so σ_0 is the dust particle cross-section times its atomic weight). A rough fit to the dust extinction in our own Galaxy is that the cross-section of cosmic dust varies approximately linearly with frequency from the infrared to the far ultraviolet. Using this approximation we adopt a fit to the data of Howarth (1983) with $\sigma_0\chi=2.7\times10^{-25}\,\mathrm{m}^2$ for the interstellar medium in our own Galaxy. It is believed that $\chi\approx0.01$ in our Galaxy, so that if the Population III era dust had the same properties σ_0 would be $2.7\times10^{-23}\,\mathrm{m}^2$. This is the only reasonable assumption we can make, but of course the size and composition of Population III grains might be quite different.

4.2 THE MASS-LOSS ATMOSPHERE

We shall consider two different forms for $n(r)$: an inverse square law corresponding to a mass-loss atmosphere, and then (in Section 4.3) $n(r)=$constant corresponding to a homogeneous nebula around the star. First we consider the star's mass-loss atmosphere. If the total mass lost in the main-sequence phase is a fraction β of the stellar mass M, the mass loss rate is $\dot{M}=\beta M/t_{\mathrm{ms}}$. Consider an r-independent wind velocity $v=10^3 v_3\,\mathrm{km\,s^{-1}}$ giving a density profile for the hydrogen number density of

$$4\pi v m_{\mathrm{H}} r^2 n=\frac{\beta Y_{\mathrm{H}} M}{t_{\mathrm{ms}}} \tag{4.3}$$

where Y_{H} is the hydrogen mass fraction. The ratio of ionizations to recombinations in the gas is then

$$\frac{\dot{N}}{4\pi\alpha n_0^2 r_0^3}=7\times10^1 M_2^{-1/2}T_5^{0.8}(\beta Y_{\mathrm{H}})^{-2}v_3^2\frac{r_0}{r_*}f_N f_t^{3/2}f_\varepsilon^{1/2}f_T^{-2} \tag{4.4}$$

where n_0 is the density at the inner edge r_0 of the $1/r^2$ nebula and the stellar radius is

$$r_*=2.8\times10^9 f_\varepsilon^{1/2}f_t^{-2}M_2^{1/2}\,\mathrm{m}. \tag{4.5}$$

Even if β is of order unity, as is likely for such radiation-pressure-dominated stars, this means that condition (4.1) cannot be easily satisfied and the envelope will be highly ionized. The main source of opacity will then be dust. Hoyle, Solomon & Woolf (1973) pointed out that massive stars might fail to produce H II regions if their ionizing continuum were absorbed by dust in their mass-loss envelope. The optical depth is just $\tau=n_0\sigma_0\chi r_0$, or

$$\tau=7.0\times10^5\chi M_2^{1/2}\beta Y_{\mathrm{H}}\left(\frac{r_0}{r_*}\right)^{-1}f_t^{-1/2}f_\varepsilon^{-1/2}f_T^2 \tag{4.6}$$

at the Lyman limit. Hence the stars can only be infrared objects if they have such a mass-loss atmosphere with $\chi\beta$ greater than about 10^{-6}. The first-generation Population III stars will have smaller abundances than this if their nucleosynthesis products are not well mixed into the atmosphere. If there is enough dust, the spectrum will be redshifted to the present epoch without

© Royal Astronomical Society • Provided by the NASA Astrophysics Data System

1986MNRAS.223..763M

further modification unless the intergalactic dust abundance is very high (see Section 4.5). For the remainder of this section we consider the case where the star is an ultraviolet source.

4.3 THE LOCAL NEBULA

We now consider a constant-density region around the star (or a group of the stars). The minimum density required to absorb all the ionizing radiation is, from equation (4.1),

$$n=\frac{\dot{N}m_{\mathrm{H}}}{\beta Y_{\mathrm{H}}\alpha_{\mathrm{eff}}M}$$
$$=2.4\times10^{10}T_5^{0.8}(\beta Y_{\mathrm{H}})^{-1}f_N\,\mathrm{m}^{-3}. \tag{4.7}$$

For dust absorption, $\tau_0=n\sigma_0\chi r$. Since we can find r in terms of n and β from $4\pi nr^3/3=N$, $\tau_0>1$ if

$$n>5\times10^4(\beta Y_{\mathrm{H}})^{-1/2}\chi^{-3/2}M_2^{-1/2}\,\mathrm{m}^{-3}. \tag{4.8}$$

In the cosmological context it is useful to express these results in terms of the corresponding cosmological density parameters and the overdensity compared with the background gas density. In this way we determine whether the condition for ionization derived in equation (4.7) requires that the entire Universe be ionized by the stars.

Assume that the mean number of stars per unit volume is n_*, and that each is surrounded by a nebula of volume V_N and gas density n_{g}. The stars may be grouped in clusters of N_* objects, in which case the total volume of the surrounding nebula is taken to be N_*V_N. Then the clumping factor δ of the nebulae, defined by the inverse of their volume-filling factor in the universe, is given by

$$\delta=\frac{n_*^{-1}}{V_N/N_*}=\frac{nm_{\mathrm{H}}}{\beta Y_{\mathrm{H}}Mn_*}. \tag{4.9}$$

Let the cosmological density parameters for the stars and nebulae be Ω_* and $\Omega_{\mathrm{g}}=\beta\Omega_*$ respectively. The corresponding coordinate number densities are

$$n_*=\frac{\Omega_*\varrho_{\mathrm{c}}(1+z)^3}{M}$$
$$=2.4\times10^{-59}\Omega_*h_{50}^2z^3M_2^{-1}\,\mathrm{m}^{-3}. \tag{4.10}$$

$$n_{\mathrm{g}}=\frac{\Omega_{\mathrm{g}}\varrho_{\mathrm{c}}(1+z)^3Y_{\mathrm{H}}\delta}{m_{\mathrm{H}}}$$
$$=2.8\,\Omega_{\mathrm{g}}h_{50}^2Y_{\mathrm{H}}\delta z^3\,\mathrm{m}^{-3}. \tag{4.11}$$

Therefore to avoid ionizing the Universe we require, substituting (4.9) in (4.7),

$$\delta>\frac{\dot{N}}{\alpha n_*}\left(\frac{m_{\mathrm{H}}}{\beta Y_{\mathrm{H}}M}\right)^2=8.3\times10^9T_5^{0.8}f_N\beta^{-2}Y_{\mathrm{H}}^{-2}\Omega_*^{-1}h_{50}^{-2}z^{-3}. \tag{4.12}$$

For the unclumped background gas, δ is unity. If equation (4.12) is to be satisfied in this case, we must choose not only large z but also large β. Assuming that we believe that the total density parameter is at most unity, this means that Ω_* must be small. Even at $z=100$ the background gas will be ionized unless Ω_* is roughly as small as 10^{-4} or so. At lower redshifts it is even easier to ionize the gas. We are interested in the case in which Ω_* is the major baryonic

© Royal Astronomical Society • Provided by the NASA Astrophysics Data System

1986MNRAS.223..763M

contributor to Ω_0, and so $\beta \leqslant 1$. We therefore conclude that a substantial amount of matter is required in dense clumped ($\delta \gg 1$) regions, or the Lyman continuum will not be absorbed (Carr *et al.* 1984).

The dust in the nebulae is optically thick to the ionizing radiation at the Lyman limit if

$$\delta > 2\times 10^4 (\beta Y_{\rm H}\chi)^{-3/2} M_2^{-1/2} \Omega_*^{-1} h_{50}^{-2} z^{-3}. \tag{4.13}$$

Equation (4.12) may be satisfied for high-redshift sources ($z \approx 100$) in the case of parent gas clouds of $10^6 M_\odot$ collapsing shortly after recombination and forming clusters of Population III objects at a later epoch. Such density perturbations would collapse and virialize, increasing their density by a factor of 40 over that which they had at binding. This density would then be a further factor of 10^3 higher than the ambient density at $z=100$, giving $\delta \approx 10^4$ which is comparable with the critical value of δ for that redshift. Normal galactic densities would be insufficient, but the densities found in dense molecular cloud cores would be adequate. The opacity from dust is similar if the gas-to-dust ratio is 1 per cent of galactic, corresponding to Population II metallicities.

4.4 ABSORPTION BY NEUTRAL HYDROGEN IN THE UNIVERSE

If equation (4.12) or (4.13) is not satisfied for the gas surrounding the VMOs, the ionizing radiation from the VMOs will ionize the Universe completely. However, even though the recombination time is not short enough for the hydrogen to absorb all the photons within the lifetime of the stars, they may still be absorbed after the sources have turned off. Since the stars emit a total of $\dot{N} t_{\rm ms}$ photons, the Universe will be filled with a photon number density $\dot{N} t_{\rm ms} n_*$. A photon travelling through clumps of density n with a volume-filling factor δ^{-1} will spend a fraction $1/\delta$ of its time in clumps, so in a time t its path length through the dense gas is ct/δ and the optical depth is

$$\tau = \frac{(1-x) n \sigma_{\rm H} c t}{\delta}. \tag{4.14}$$

There are $\tau \dot{N} t_{\rm ms} n \dot{N}/t$ ionizations per unit volume per unit time in the gas. Equating this to the number of recombinations in the gas gives a total photon optical depth for time t of

$$\tau = \frac{\alpha n^2/\delta}{\dot{N} n_*} \frac{t}{t_{\rm ms}}, \tag{4.15}$$

so that $\tau > 1$ if

$$\delta > \frac{\dot{N}}{\alpha n_*} \left(\frac{m_{\rm H}}{\beta Y_{\rm H} M} \right)^2 \frac{t_{\rm ms}}{t}. \tag{4.16}$$

If $t = t_{\rm ms}$ we recover the previous analysis (equation 4.12). If t is the expansion time, we obtain the condition that the ionizing continuum be absorbed before it redshifts below the threshold:

$$\delta > 2.2\times 10^6 T_5^{0.8} (\beta Y_{\rm H})^{-2} (\Omega_* h_{50}^2)^{-1} (\Omega_0 h_{50}^2)^{1/2} (1+z)^{-3/2} f_N f_t^{-1}. \tag{4.17}$$

If the photons cannot be absorbed within a time of the order of the expansion time, the bulk of the photons will be redshifted below the Lyman limit without being absorbed. Hence the spectrum may reach us largely unaltered if the gas associated with the VMOs is not so highly clumped that its recombination time is very short, the clumpiness being given by δ above.

© Royal Astronomical Society • Provided by the NASA Astrophysics Data System

1986MNRAS.223..763M

The ionization of the clumps is found to be given by

$$1-x=\frac{\alpha}{\dot{N}\sigma ct_{\rm ms}}\frac{\beta Y_{\rm H}M}{m_{\rm H}}\delta$$
$$=2\times10^{-12}\delta(T_5^{-0.8}\beta Y_{\rm H}f_N^{-1}f_t^{-1}). \qquad (4.18)$$

Couchman (1985) has studied the effects of a smaller abundance of VMOs on the thermal history of the intergalactic medium.

4.5 DUST ABSORPTION IN THE UNIVERSE

Now let us consider the effects of dust in the Universe as the photons are redshifted to the present epoch. There will be absorption due to both any dust in a uniform intergalactic medium and dust in galaxies along the line-of-sight. As pointed out by Ostriker & Heisler (1984), the patchiness of the latter effect may allow it to obscure high-redshift objects without the revealing presence of partially obscured objects at lower redshifts. The obscuration is uncertain owing to our lack of knowledge of the evolution of dust content in galaxies and of the size of the absorbing region in a typical galaxy. Ostriker & Heisler pointed out that in an exponential disc galaxy the radius corresponding to a given optical depth through the disc will increase at high redshift owing to the increase in dust opacity with the frequency of the photon. This leads to very high effective cross-sections for high-redshift galaxies and a high covering factor of the galaxies on the sky at a given redshift. However, it is not clear that the gas and dust distribution in galaxies follows the light distribution in this way. In fact modern observations indicate (Blitz, Fich & Kulkarni 1983) that the hydrogen surface density in our Galaxy is fairly constant out to a radius of 20 kpc and then cuts off sharply. Of course, it may just be that the hydrogen is ionized beyond this point, but the warping and scalloping of the disc in this region suggests that the Galaxy may have a recognizable edge rather than just going on for ever. Provided that the dust-to-gas ratio does not increase with galactocentric radius, this density profile will result in a galaxy effective radius that is constant with redshift (although the optical depth through a given galaxy will still increase, the covering factor due to galaxies will not be so large). At high redshifts more of the mass of a galaxy may be in diffuse form than at our epoch, but the dust-to-gas ratio may be smaller and the size of the dusty region may be smaller if infall and collapse are not complete. We therefore believe that the covering factor calculated below (equation 4.19) is not an unreasonable estimate. At the Lyman edge, neutral hydrogen absorption will be more important than dust (at a normal dust-to-gas ratio of order 10^{-2}) provided that the neutral fraction is more than 5×10^{-4}. Within an expansion time of the Population III era when the Universe might be filled with large numbers of ionizing photons the neutral fraction could be significantly less than this, so that dust might still be the most important opacity source even at the high frequencies of the peak of the background spectrum.

We adopt representative values of galaxy radius $r=20$ kpc, area $A_{\rm G}=\pi r^2$, disc thickness $H=200$ pc, optical depth through the disc $\tau_{\rm G}(\nu)=\sigma(\nu)\chi nH=0.5(\chi/0.01)(\nu_{15})$, where $\nu=10^{15}\nu_{15}$ Hz, and comoving galaxy number density $n_{\rm G}=0.01\,{\rm Mpc}^{-3}$.

Consider a disc galaxy at an angle θ to the line-of-sight; it has projected area $A_{\rm G}\cos\theta$, and there are $n_{\rm G}d(\cos\theta)$ such galaxies per unit volume, each with optical depth along the line-of-sight $\tau_{\rm G}(\nu)\sec\theta$. The covering factor is then

$$N=\tfrac{1}{2}n_{\rm G}A_{\rm G}cH_0^{-1}\int_0^z(1+z)^{1/2}dz$$
$$=0.025\,h_{50}^{-1}[(1+z)^{1.5}-1] \qquad (4.19)$$

© Royal Astronomical Society • Provided by the NASA Astrophysics Data System

1986MNRAS.223..763M

[in agreement with Bond *et al.* (1985)] and the optical depth along the line-of-sight at comoving frequency $\nu_0 = 10^{15}\nu_{15}$ Hz is

$$\tau(\nu_0, z) = n_G A_G \tau_G(\nu_0) c H_0^{-1} \int_0^z (1+z)^{1.5} dz$$

$$= 0.015\nu_{15} \frac{\chi}{0.01} h_{50}^{-1}[(1+z)^{2.5}-1], \tag{4.20}$$

assuming that z is large enough that there are always several galaxies lalong the line-of-sight, i.e. $N>1$ or $z>11$.

For the uniform intergalactic medium the optical depth may be quite large. Limits from reddening in quasi-stellar objects (Wright 1981) suggest that any intergalactic dust has $\Omega_d < 1.2\times10^{-4} h_{50}^{-1}$. Assuming this maximum amount gives

$$\tau(\nu, z) = 0.25\nu_{15} h_{50}{}^{-1}[(1+z)^{2.5}-1]. \tag{4.21}$$

Hence in the worst case the optical depth due to a dusty intergalactic medium could be substantially larger than that due to galaxies. At high redshifts such an obscuration would be of great importance. The Lyman limit is at a comoving frequency of $\nu_{15} = 3.3(1+z)^{-1}$, corresponding to an optical depth from equation (4.21) of $0.8z^{1.5}$ at large z. This would completely obscure sources at high redshifts. However, this assumes that the dust existed at these redshifts. If the Population III objects form well before galaxy formation, the upper limit in the integral should probably be the redshift of galaxy formation rather than of the sources. In summary, it appears impossible to resolve the issue of whether or not cosmological dust absorption is important at present. In later sections we present results assuming no dust, dust forming at $z=3$ and dust forming at the same epoch as the stars to illustrate the likely range of effects. Of course, if features in the ultraviolet background such as the postulated redshifted helium line discussed by Henry *et al.* (1978) (but not confirmed in subsequent observations) are ever demonstrated to be of cosmological origin, cosmic extinction will be severely constrained.

5 Modelling the stellar and nebular spectrum

The spectrum of a pure hydrogen nebula photo-ionized by a VMO will be largely recombination continuum and Lyman line radiation. We take into account free–bound and free–free processes, but we ignore collisional excitations and photo-ionizations from excited states. We start by omitting collisional ionization and excitation entirely, to obtain a first approximation to the problem, and then include these processes.

In the actual spectrum calculated we approximate the line spectrum by assuming that an electron recombining to an excited level falls one level at a time to the ground state, producing Lα, Hα, Pα etc. photons. This gives the correct total energy and corresponds to the standard 'case B' approximation in which the optical depth is large in the Lyman lines. We also assume that Lα line photons will be scattered out of the high optical depth line core before they are degraded.

The electron temperature of the nebula is calculated by modifying the hydrogen nebula equation of Baker, Menzel & Aller (1938) to include the on-the-spot approximation. Suppose that in a region of the nebula with emission measure $W = n^2 V$ the gas absorbs N stellar ionizing photons per unit time corresponding to absorbed energy L per unit time. Then the total number of recombinations must be equal to N plus the number of ionizing photons created in recombination and free–free processes. Hence the effective recombination rate is equal to the recombination coefficient for non-ionizing photons minus the production rate of ionizing free–free photons. Similarly, L must be equal to the emitted luminosity from non-ionizing

© Royal Astronomical Society • Provided by the NASA Astrophysics Data System

1986MNRAS.223..763M

recombination and free–free radiation. In fact, if we adopt as temperature parameter $x_0 = R/kT$, where $R = \frac{1}{2}\alpha^2 mc^2$, and define a characteristic recombination coefficient

$$A_0 = 64\pi^2(3\pi)^{-3/2}\alpha^2\left(\frac{\hbar}{mc}\right)^2 c = 5.20\times10^{-20}\,\mathrm{m^3\,s^{-1}}, \tag{5.1}$$

then

$$\frac{N}{W} = A_0 x_0^{3/2} f(x_0), \tag{5.2}$$

$$\frac{L}{W} = RA_0 x_0^{3/2} g(x_0)$$

and

$$\frac{L}{NR} = \frac{g(x_0)}{f(x_0)} = \varepsilon(x_0), \tag{5.3}$$

where $\varepsilon(x_0)$ is a completely determined function of temperature which is derived below. Choosing to express all quantities in terms of A_0 allows us to express the standard equations for the radiative processes in a particularly simple form, avoiding the usual proliferation of dimensional constants. Hence for a given value of L/NR, since $\varepsilon(x_0)$ is monotonic in the range of interest, the temperature of the zone can be determined and the spectrum calculated. L and N are both proportional to the neutral fraction, so this unknown factor cancels out and the ionization does not need to be known before the temperature. It turns out that a simple one-zone model reproduces the spectrum and the value of W required to absorb all the ionizing radiation to good accuracy when compared with more detailed zoned-ionization models run with a variety of parameters. The derived electron temperature is close to that of the input stellar spectrum.

We now derive the function $\varepsilon(x_o)$. The recombination coefficient to level n is

$$\alpha_n(x, x_0) = A_0 x_0^{3/2}\,\frac{\exp(x_0/n^2)}{n^3}\,\frac{\exp(-x)}{x} \tag{5.4}$$

for $x > x_0/n^2$, where $x = h\nu/kT = h\nu x_0/R$ is a dimensionless frequency variable. Hence the total recombination coefficient to levels $n=2$ and above, excluding recombinations which produce ionizing photons (so that the frequency integral is cut off at $x = x_0$), is

$$\alpha_{\text{non-ionizing}}(x_0) = A_0 x_0^{3/2} \sum_{n=2}^{\infty} \frac{1}{n^3} \exp\left(\frac{x_0}{n^3}\right)\left[E_1\left(\frac{x_0}{n^2}\right) - E_1(x_0)\right] \tag{5.5}$$

where E_1 is the first exponential integral

$$E_1(y) = \int_y^{\infty} \exp(-y)\,dy/y.$$

The energy emitted for each of these recombinations consists of a continuum photon of energy xR/x_0 and line photons of total energy $R(1-1/n^2)/x_0$, which is the energy level difference between level n and the ground state. The frequency-integrated emission coefficient is therefore

$$j_{\text{cont}} = RA_0 x_0^{3/2} \sum_{n=2}^{\infty} \frac{1}{n^3} x_0^{-1}\left\{1 - \exp\left[-x_0\left(1-\frac{1}{n^2}\right)\right]\right\} \tag{5.6}$$

© Royal Astronomical Society • Provided by the NASA Astrophysics Data System

1986MNRAS.223..763M

for the recombination continuum, and

$$j_{\text{line}}=RA_0x_0^{3/2}\sum_{n=2}^{\infty}\frac{1}{n^3}\left(1-\frac{1}{n^2}\right)\exp\left(\frac{x_0}{n^2}\right)E_1\left(\frac{x_0}{n^2}\right) \tag{5.7}$$

for the lines.

The free–free radiation has emission coefficient

$$j_{\text{ff}}(x)=\tfrac{1}{2}RA_0x_0^{-1/2}\exp(-x), \tag{5.8}$$

and hence the ionization coefficient due to ionizing free–free photons is

$$\alpha_{\text{ff}}=\tfrac{1}{2}A_0x_0^{1/2}E_1(x_0) \tag{5.9}$$

and the emission coefficient from the non-ionizing free–free radiation is

$$j_{\text{ff}}=\tfrac{1}{2}RA_0x_0^{-1/2}[1-\exp(-x_0)]. \tag{5.10}$$

Therefore

$$\varepsilon(x_0)=\left\langle\sum_{n=2}^{\infty}\frac{1}{n^3}\left[\!\!\left[\left(1-\frac{1}{n^2}\right)\exp\left(\frac{x_0}{n^2}\right)E_1\left(\frac{x_0}{n^2}\right)+x_0^{-1}\left\{1-\exp\left[-x_0\left(1-\frac{1}{n^2}\right)\right]\right\}\right]\!\!\right]\right.$$
$$\left.+\tfrac{1}{2}x_0^{-2}[1-\exp(-x_0)]\right\rangle\left\{\sum_{n=2}^{\infty}\frac{1}{n^3}\exp\left(\frac{x_0}{n^2}\right)\left[E_1\left(\frac{x_0}{n^2}\right)-E_1(x_0)\right]-\tfrac{1}{2}x_0^{-1}E_1(x_0)\right\}^{-1}. \tag{5.11}$$

The value of α_{eff} calculated for the blackbody VMO spectrum is $1.4\times10^{-20}\,\text{m}^3\,\text{s}^{-1}$, corresponding to $W=5.8\times10^{69}\,\text{m}^{-3}$. This corresponds to $T_5=3.3$ in equation (4.7), although the actual temperature is only of order 1×10^5 K. The resultant spectrum is plotted in Fig. 2(b). We shall refer to it as the R model. As with all the other spectra used in the numerical studies, it is stored as $\nu s(\nu)$ in bins 0.02 wide in $\log\nu$. Lines are assumed to have a width of less than 1 bin. For this model, 50 per cent of the flux is in the Lyman line. As a better approximation to the unabsorbed spectrum we adopt a pure hydrogen model stellar atmosphere (SA) from Wesemael *et al.* (1980) (Fig. 2a, compared with the blackbody model). Although intended for a degenerate star, it should be a reasonable approximation to our high-gravity Population III stars. The spectrum is harder than the blackbody in the sense that there is more ionizing energy flux for the same effective temperature, but there are few ionizing photons ($f_N=0.73$). The density required in the surrounding gas to absorb this spectrum completely above the Lyman limit is slightly higher than for the blackbody model, but the resulting spectrum is very similar. Taking into account collisional effects and two-photon emission requires substantially more computation; results (J. C. McDowell, in preparation) show that the spectrum is substantially similar but the fraction of flux in the Lyman line varies with gas density.

6 The spectrum of the background radiation

We denote by $s(\nu)\,d\nu$ the fraction of the luminosity between frequencies ν and $\nu+d\nu$ coming from the source (after modification by neutral hydrogen or dust absorption if appropriate). The intensity of the background produced is

$$i(\nu)=\frac{\varepsilon Mc^2n_*s(\nu)}{4\pi}. \tag{6.1}$$

© Royal Astronomical Society • Provided by the NASA Astrophysics Data System

1986MNRAS.223..763M

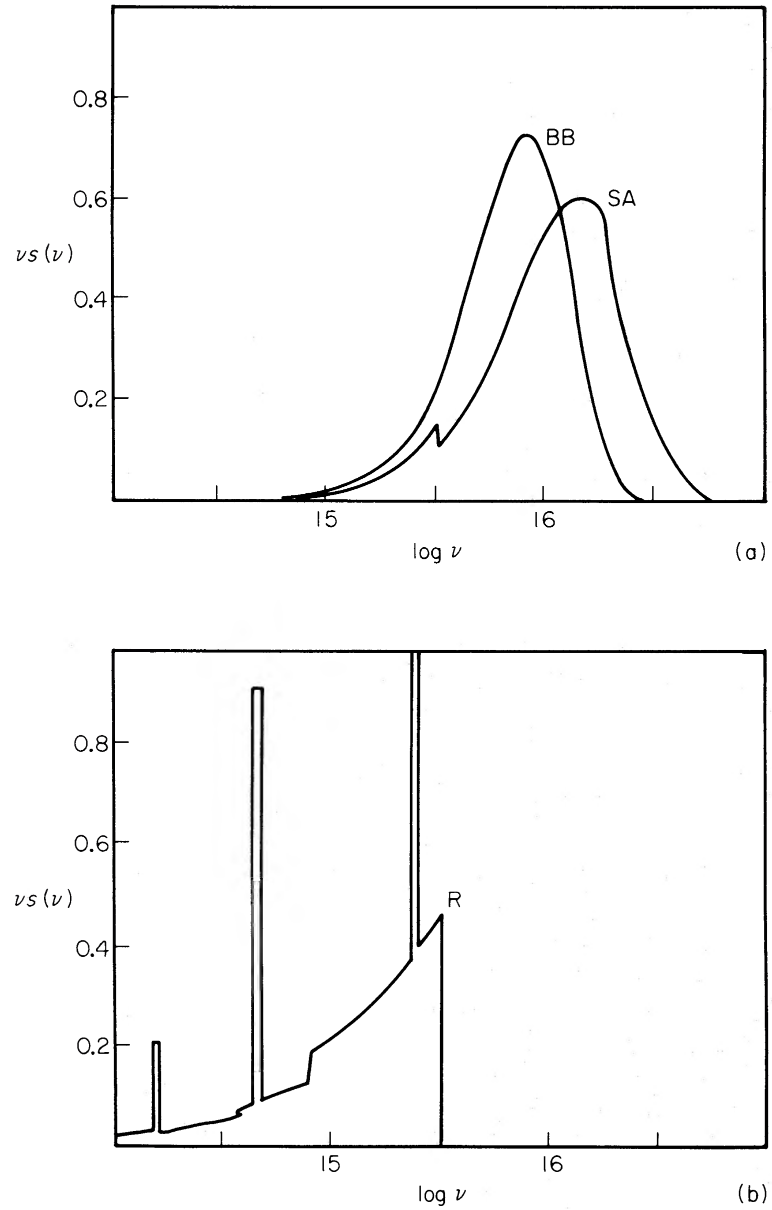

Figure 2. Model Population III VMO atmospheres. The energy per logarithmic frequency interval is plotted normalized to unit total energy: (a) the blackbody (BB) and hydrogen stellar atmosphere (SA) as described in the text; (b) the recombination model (R) calculated as described in the text for a star hidden by a dense hydrogen nebula.

We represent the radiation field energy density by the dimensionless parameter

$$\omega(\nu)=\frac{4\pi\nu i(\nu)}{\varrho_c c^3} \tag{6.2}$$

$$=\varepsilon\Omega_*(1+z)^3\nu s(\nu).$$

To enable us to work in comoving frequency we define

$$\omega_0(\nu,z)=\omega[\nu(1+z),z](1+z)^{-4}. \tag{6.3}$$

Then, if the background radiation is produced at redshift z and evolves without modification as

© Royal Astronomical Society • Provided by the NASA Astrophysics Data System

1986MNRAS.223..763M

the Universe expands,

$$\omega(\nu, 0)=\omega_0(\nu, z)$$
$$=\varepsilon\Omega_* \nu s[\nu(1+z)]. \tag{6.4}$$

It is also related to the total cosmological density parameter of the radiation by

$$\Omega_R=\int \omega(\nu)\, d(\ln \nu). \tag{6.5}$$

For comparison, the value of $\Omega_R h_{50}^2$ for the microwave background is 10^{-4}. The present value of $\omega(\nu)$ can in principle be determined by observation, and adoption of a model $s(\nu)$ immediately leads to Ω_*, the mass in VMOs. In practice attempts to detect and measure extragalactic background light are very difficult indeed, and all observations will be treated as upper limits, yielding upper limits for the maximum possible mass in an early generation of very massive stars.

If we take into account the absorption due to the intergalactic medium or consider Population III star formation over an extended redshift range, we must solve the radiative transfer problem. Negroponte (1986) has studied the evolution of the dust temperature with redshift in a universe heated by such pregalactic sources using a detailed radiative transfer code, and has shown that the dust temperature is significantly affected by the choice of dust opacity law. We have calculated the background radiation spectrum using a similar code which should be sufficiently accurate for the present investigation. Our code incorporates a background spectrum covering any given frequency range, but we have used a spectrum covering the range $\nu=10^{10}$–10^{17} Hz in comoving frequency. The values of $\omega_0(\nu, z)$ are stored in an array with bin size equal to 0.02 in $\log \nu$. The redshift evolution in frequency is treated simply by altering the origin of the array index at each redshift step.

The inputs to the code include the input source spectrum model, which for this discussion is one of the Population III models discussed in Section 2 but in principle could be the normalized spectrum of any supposed radiation source. The parameters of the source are defined by specifying its lifetime and efficiency ε. The cosmological model is specified by Ω_0 and H_0 to describe the overall Friedmann universe, Ω_* and z_* to define the density parameter and formation redshift of the sources, and Ω_d and z_d to define the density parameter and formation redshift of the dust. The dust opacity law can also be selected, and is discussed below. Finally an initial integration step size is chosen; the redshift parameter used is $\zeta=\log(1+z)$ and the step size for the part of the run is a constant increment in ζ.

Before running the code the spectrum is initialized and a 3 K blackbody can be added to the spectrum to represent the microwave background. The code evolves the spectrum from the initial value of $\zeta=\log(1+z_*)$ to $\zeta=0$. The cosmological time t is evaluated at each step and the size of the integration step in time dt is also evaluated. In each step the contribution from the stellar radiation is added in provided that $t+dt<t_*+t_{ms}$. If the stars expire within a particular step their contribution within that step is reduced by the appropriate proportion. In this way the code can treat star which have lifetimes longer than the expansion time and we are not restricted to the instantaneous approximation used earlier.

If $z<z_d$ the step size for the zone is changed so that the optical depth to the dust is only 0.1 for the zone at the highest frequency at which the flux in the background is non-zero. The code now calculates the dust absorption and emission as described below.

The observationally determined parameters needed to normalize our dust opacity law are first the dust optical depth at V per unit hydrogen column in our Galaxy, found from the optical depth per unit distance C_V compared with the mean hydrogen density n; secondly the dust-to-gas mass ratio χ_{Gal} in our Galaxy and finally the variation in optical depth with frequency. This is

© Royal Astronomical Society • Provided by the NASA Astrophysics Data System

1986MNRAS.223..763M

traditionally expressed in terms of the selective extinction $A_\lambda/E(B-V)$ which is the ratio of total extinction at λ to the selective extinction of B relative to V. We normalize the optical depth to the value of the extinction optical depth at a fiducial frequency $\nu_P=10^{15}$ Hz, denoting this dimensionless cross-section by $\sigma(\nu)=\tau(\nu)/\tau(\nu_P)$, and convert from selective extinction using the ratio $R=A_V/E(B-V)$. To obtain the absorption optical depth relevant to the background light calculation, where scattering has no net effect, we must multiply the extinction value by $1-F_\nu$, where F_ν is the frequency-dependent dust albedo. Hence the value of σ as defined here is not unity at ν_P in this case. These quantities enable us to calculate the dust optical depth for a given dust mass column if it is assumed that the nature of the dust particles is the same as in our Galaxy. We have

$$d\tau(\nu)=(1-F_\nu)\frac{A_\lambda}{RE(B-V)}\frac{C_V}{n\chi_{\mathrm{Gal}}m_{\mathrm{H}}}\varrho_{\mathrm{d}}\,dr=\varkappa_{\mathrm{P}}\varrho_{\mathrm{d}}\,dr \tag{6.6}$$

for intergalactic dust of density ϱ_{d} over coordinate path length dr.

We adopt (Spitzer 1978) $R=3.2$, $C_V=1.9\,\mathrm{mag\,kpc^{-1}}$, $n=1.2\,\mathrm{cm^{-3}}$, $\chi_{\mathrm{Gal}}=0.01$ and $A_{\mathrm{P}}/E(B-V)=5.8$; then $\varkappa_{\mathrm{P}}=5700\,\mathrm{m^2\,kg^{-1}}$ and

$$d\tau(\nu)=4.9\times10^3\,\Omega_{\mathrm{d}}h_{50}(1+z)^3\sigma[\nu(1+z)]\frac{d(H_0t)}{dz} \tag{6.7}$$

for an element of look-back time dt, giving a total optical depth

$$\tau(\nu)=4.9\times10^3\,\Omega_{\mathrm{d}}h_{50}\int(1+z)^3\frac{d(H_0t)}{dz}\sigma[\nu(1+z)]\,dz. \tag{6.8}$$

For the frequency dependence of the absorption we have adopted the extinction law calculated by Draine & Lee (1984) for a graphite and silicate mixture. In the optical and ultraviolet we have used the values for the extinction tabulated by Savage & Mathis (1979) rather than the curve calculated by Draine & Lee to fit these values, but we have used Draine & Lee's estimate of the albedo at all frequencies to estimate the absorption from the extinction. The extinction in the extreme ultraviolet is completely uncertain; it must flatten off at some wavelength of the order of the smallest grain size but it is still rising at 1000 Å. We choose our opacity law to be linear up to the Lyman limit at 3.3 PHz and constant beyond this value. At low frequencies ($\nu<0.01$ PHz) we have adopted a ν^2 law in agreement with the Draine & Lee model.

To evaluate the dust temperature in each redshift zone, we evaluate the absorbed energy

$$\varrho_{\mathrm{A}}=\int\sigma(\nu)f(\nu)\,d(\nu) \tag{6.9}$$

where f is the spectral energy density (in $\mathrm{J\,m^{-3}}$), and compare it with a look-up table of the energy $\varrho_{\mathrm{E}}(T_{\mathrm{d}})$ emitted (the same integral evaluated using a Planck distribution at temperature T_{d}). The dust temperature is always at least 3 K because of the microwave background and cannot exceed some melting point T_{melt}. The appropriate value of T_{melt} is unclear but we arbitrarily adopt $T_{\mathrm{melt}}=2000$ K (the dust is never this hot in practice) and evaluate 200 values of ϱ_{E} equally spaced in log T_{d} between these temperature limits. Linearly interpolating between these values to find T_{d} for a given ϱ_{A} gives energy conservation to sufficient accuracy at each step to ensure that the total energy remains constant to 1 per cent in the whole integration.

Since the neutral hydrogen in the intergalactic medium cannot have a large optical depth (equation 4.17 with $\delta=1$) we only consider the absorbing effects of dust, which is assumed to reach a steady state on time-scales much shorter than the expansion time.

Some approximate results can be derived analytically, and agree qualitatively with the numerical calculations. If the epochs of Population III and dust formation are t_* and t_{d}

© Royal Astronomical Society • Provided by the NASA Astrophysics Data System

1986MNRAS.223..763M

respectively, t_0 is the present and $z=z(t)$, then

$$\omega(\nu,0)=\omega_0[\nu,z(t_*)]+\int_{t_*}^{t_0}[F_*(\nu,t)+F_{\rm d}(\nu,t)]\,dt \tag{6.10}$$

and the source terms are

$$F_*(\nu,\,t)=\frac{\varepsilon\Omega_*\nu s[\nu(1+z)]}{t_{\rm ms}}, \tag{6.11}$$

and for $t>t_{\rm d}$

$$F_{\rm d}(\nu,t)=n_{\rm g}\sigma[\nu(1+z)]\chi c\{\omega_{\rm eq}[T,\nu(1+z)](1+z)^{-4}-\omega_0(\nu,z)\} \tag{6.12}$$

where the dust temperature T is found from

$$\int F_{\rm d}(\nu)\,d(\ln\nu)=0 \tag{6.13}$$

and the dust emission follows a Planck distribution

$$\omega_{\rm eq}(T,\,\nu)=\frac{8\pi h}{\varrho_{\rm c}c^5}\,\frac{\nu^4}{\exp(h\nu/kT)-1} \tag{6.14}$$

modified by the dust cross-section. Now we adopt the approximation that $\sigma(\nu)=\sigma_0(\nu/\nu_0)$,

$$\int\frac{\sigma(\nu)\,\nu^3}{\exp(h\nu/kT)-1}=4!\,\zeta(5)\left(\frac{kT}{h}\right)^5\frac{\sigma_0}{\nu_0}, \tag{6.15}$$

which allows us to find T explicitly in terms of the incident spectrum

$$T^5=0.04\left(\frac{h}{k}\right)^5\frac{\varrho_{\rm c}c^5}{8\pi h}\int\omega(\nu,z)\,d\nu. \tag{6.16}$$

Of course, the microwave background should be included in the initial spectrum $\omega_0[\nu,\,z(t_*)]$; the dust temperature then never drops below $3(1+z)$ K.

If the heating is mainly due to the VMOs, the blackbody model spectrum at temperature $10^5 f_T$ K predicts a redshifted dust temperature

$$\frac{T}{1+z_{\rm d}}=45(f_\varepsilon f_T\Omega_*)^{1/5}(1+z_*)^{-2/5}\,{\rm K} \tag{6.17}$$

for dust at $z_{\rm d}$ heated by stars at z_*. The prediction of Bond *et al.* (1986) with a more complicated dust model can be rewritten as

$$\frac{T}{1+z_{\rm d}}=29(f_\varepsilon\,\Omega_*)^{1/5}(1+z_{\rm d})^{-1/5}(1+z_*)^{-1/5}\,{\rm K}.$$

Hence the expected spectrum is a background at a few hundred microns, fairly independently of the details of the heating model.

If we assume that the stellar radiation and dust emission do not overlap in frequency, then above some comoving frequency ν_1

$$\omega_0(\nu,z)=\omega_0(\nu,z_{\rm d})\exp[-\tau(\nu,z)]. \tag{6.18}$$

We treat the case where the universe is optically thin to the dust emission, so that τ is small for

© Royal Astronomical Society • Provided by the NASA Astrophysics Data System

1986MNRAS.223..763M

$\nu<\nu_1$. In this case we can write

$$\int_0^\infty \varkappa[\nu(1+z)]\omega_0(\nu, z)\,d(\ln \nu)=\frac{15}{\pi^4}\frac{\varepsilon\Omega_*}{1+z_*}\frac{kT_*}{h(1+z_*)}(1+z)\,I[\lambda(z)], \tag{6.19}$$

where we can describe the redshift dependence of the optical depth τ between z_* and z by writing it as

$$\tau(z)=\frac{h\nu(1+z_*)}{kT_*}\lambda(z)$$

and where the integral

$$I(\lambda)=\int_0^\infty \frac{y^4\exp(-\lambda y)\,dy}{\exp(y)-1} \tag{6.20}$$

can be expressed in terms of the hexagamma function $\psi^{(4)}(x)$ (Abramowicz & Stegun 1965):

$$I(\lambda)=-4!\,\psi^{(4)}(1+\lambda)=4!\sum_{k=0}^{\infty}(\lambda+k)^{-5}. \tag{6.21}$$

Note that $I(0)=4!\,\zeta(5)$ as expected. Hence the temperature at a later epoch z is reduced by a factor

$$\left\{\frac{1}{\zeta(5)}\sum_{k=0}^{\infty}[\lambda(z)+k]^{-5}\right\}^{1/5} \tag{6.22}$$

where the optical depth between z_* and z is proportional to λ as defined above.

If the stars form over an extended redshift range, then in general the most recent epoch will dominate owing to the $1+z$ fall-off in energy. However, for the recombination spectrum model we can make a useful approximation; if we consider just the Lyman α line (which contains half the flux in our simple model), then the intensity of the background at a particular frequency is simply proportional to the star formation rate per unit redshift $\phi(z)$ evaluated at the redshift at which the line has that comoving frequency. Thus an observed set of limits as a function of frequency can be directly inverted to give a limit on $\phi(z)$ (Carr, McDowell & Sato 1983).

Figs 3 and 4 show the calculated spectrum for a variety of models superimposed in the background light constraints and the 3 K blackbody representing the microwave background. All the models were run with $h_{50}=1$, $\Omega_*=0.1$, $f_\varepsilon=1$ and $s(\nu)$ equal to either the blackbody (Fig. 3) or recombination (Fig. 4) models described in Section 4. In Fig. 3(a) the stars form at $z=40$. The full curves show the spectrum in a dust-free universe, and the broken curves show the effects of adding dust (equal to the maximum observationally allowed amount of $\Omega_d=10^{-4}$) at redshifts less than 3, causing a small far-infrared background at several hundred microns. Doing the same thing to stars which form at $z=3$ (Fig. 3b) is far more spectacular – their higher frequency in the dust's rest frame means that the opacity is higher, and so is the dust temperature. This produces a large peak in the far infrared. Putting in both dust and stars at $z=40$ produces only a distortion in the microwave background; all the stellar spectrum is absorbed at high redshifts and the dust temperature cools to the microwave temperature by the present epoch. This last spectrum has not been plotted.

Fig. 4 shows the same sequence of models but with the recombination source spectrum. Since this is at lower frequencies the effects of dust are less marked. The dotted curve in Fig. 4(a) shows the effect of dust absorption from $z=40$ to the present with a smaller dust abundance

© Royal Astronomical Society • Provided by the NASA Astrophysics Data System

1986MNRAS.223..763M

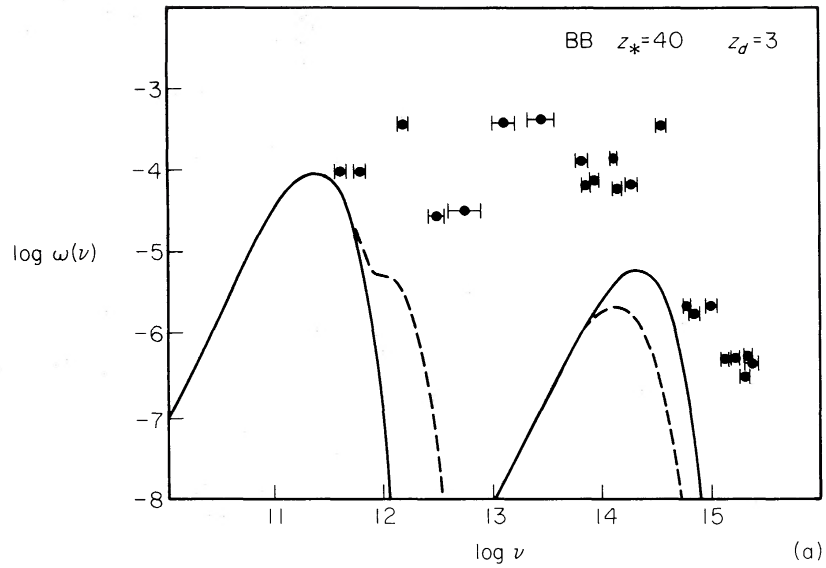

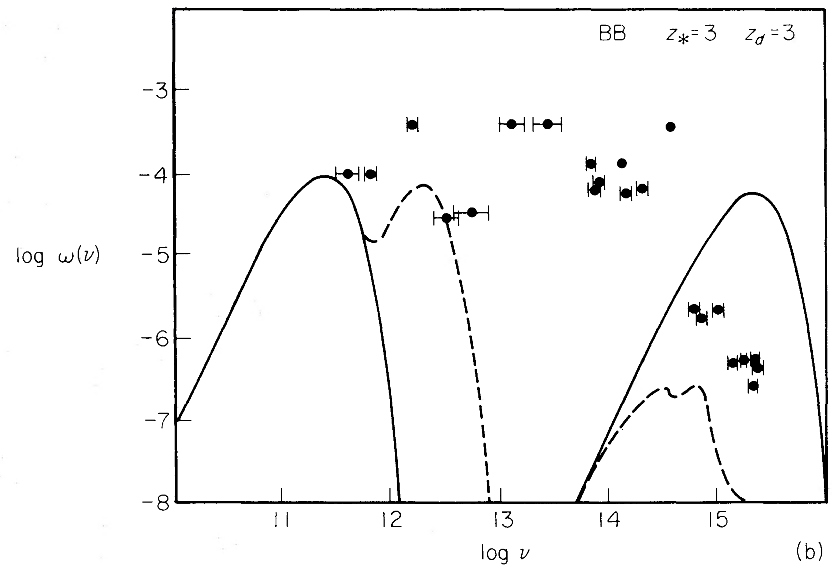

Figure 3. Predicted background spectra for blackbody sources. The full curves show the predicted spectra for Population III stars having $\Omega_*=0.1$ at $z=40$ (a) and at $z=3$ (b). The left-hand curve is the microwave background and the right-hand curve is the radiation from the stars. Some of the observational limits are superimposed for comparison. The broken curves in each case show the effect of filling the Universe with dust having $\Omega_d=10^{-4}$ forming at $z=3$.

$\Omega_d=2.5\times10^{-5}$; a highly degraded remnant of the original spectrum contributes in the *IRAS* infrared, while there is a substantial microwave distortion.

7 The constraints from background light limits

We now compare the predicted spectra of Section 6 with the observational limits. To compare a given predicted spectrum with a particular observational limit, we estimate the average value of $\omega(\nu)$ within the estimated bandpass of the observation (after first subtracting the microwave background if appropriate); the bandpass transmission is modelled as a simple box function between the two values of log ν defining the bandwidth. In some cases a triangular transmission

© Royal Astronomical Society • Provided by the NASA Astrophysics Data System

1986MNRAS.223..763M

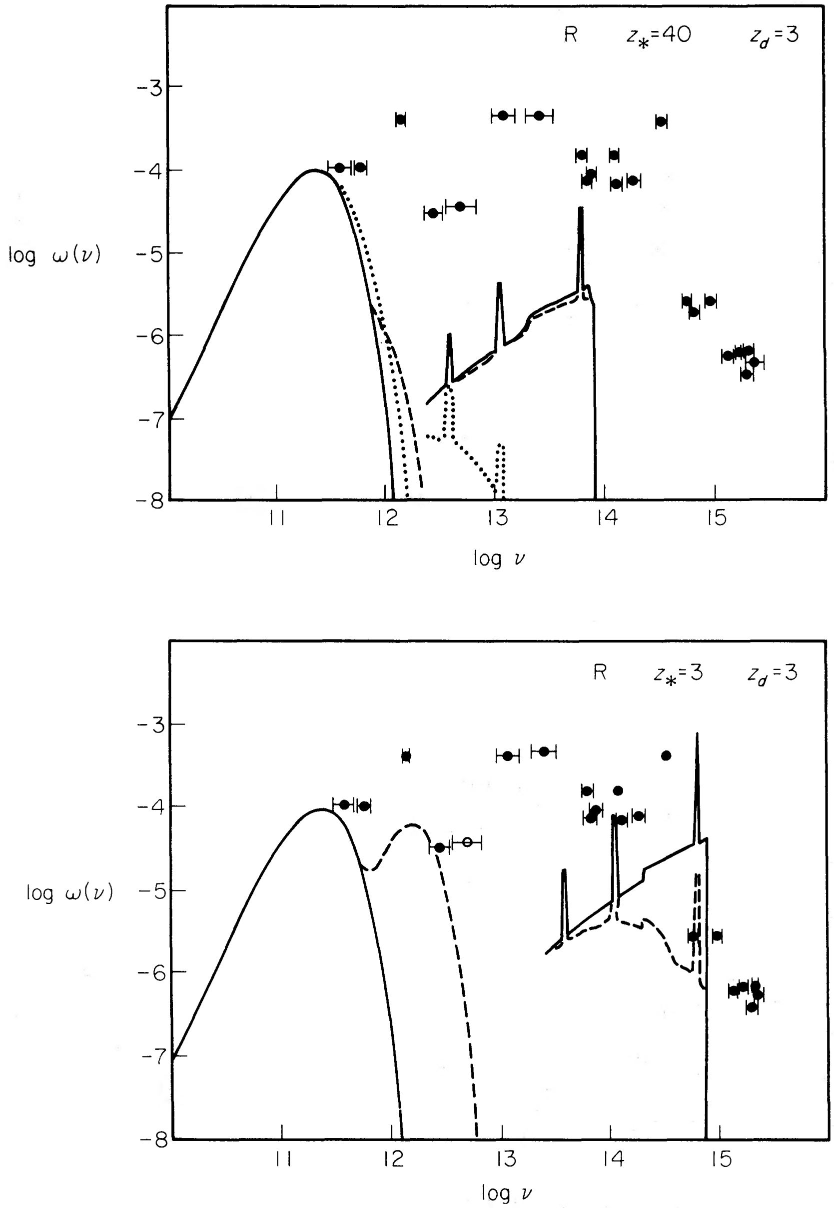

Figure 4. Predicted background spectra for the R model. These diagrams repeat the scenario of Fig. 3, but with the sources having an R model spectrum rather than a blackbody spectrum. In addition, the dotted curve in (a) shows the spectrum for the smaller dust abundance $\Omega_d = 2.5 \times 10^{-5}$ but with the dust forming at $z = 40$.

function might have been a better model but the simple rectangular model was adopted for simplicity and uniformity. The shape of the transmission function of the observational data will only be important for the R model spectrum, where the strong Lyman α line may give a strong observed signal even if it is far from the effective wavelength of the observation. In this context it is worth noting that many of the observations are quite broadband. Once the estimated value of $\omega(\nu)$ has been evaluated, it can be compared with the value in Table 1. Since the flux is proportional to Ω_*, the ratio of the two values immediately gives the maximum value of Ω_* consistent with the observations. (Actually, we might worry that this may be false in some of the models with dust. If the dust temperature is dominated by the microwave background radiation at small Ω_*, but by the stars at large Ω_*, the dust emission spectrum will not be simply proportional to Ω_*. This should be a minor effect except for very small Ω_*.)

© Royal Astronomical Society • Provided by the NASA Astrophysics Data System

1986MNRAS.223..763M

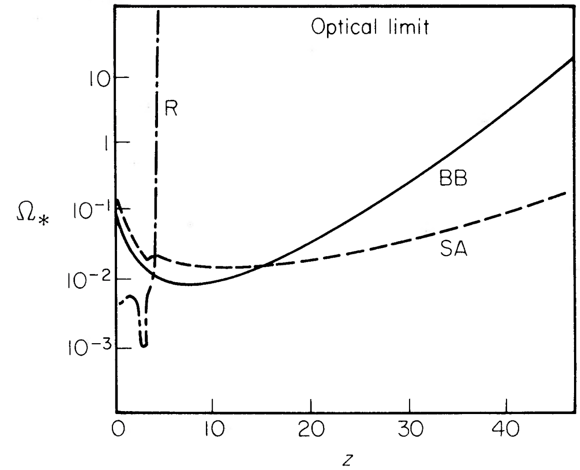

Figure 5. Single-frequency limit. This diagram shows the maximum Ω_* that does not produce a background exceeding the 4400 Å limit as a function of redshift for the three spectral models.

For each spectrum we repeat this procedure for each of the observational limits, and take the smallest limit on Ω_* from any of the observational points. Which point gives the best limit will depend on the assumed star formation redshift z_*; lower redshifts will mean that the spectra peak at higher frequencies and so the points giving the most sensitive limit will be the high-frequency ones.

To illustrate the form of the results, Fig. 5 shows the derived upper limits on Ω_* for a single observational point, the 4400 Å point of Toller (1983). The limits displayed are for all spectral models (BB, SA and R) in a dust-free universe. The limits are strongest where the peak of the spectrum is redshifted to the wavelength of the observation. For BB model the limits are weak at low z because the observation probes the Rayleigh–Jeans tail of the spectrum; the high-z limits are weak because the bulk of the spectrum has been redshifted past the visible into the infrared if the redshift is high. The stellar atmosphere model SA provides a stronger constraint at higher redshifts because the corresponding spectrum is harder than a blackbody spectrum. The R model gives a very strong limit for the redshift range in which the Lyman α line lies within the bandpass of the observation, but gives no constraint at redshifts large enough that the Lyman cut-off is redward of the observed wavelength (Carr *et al.* 1984).

The corresponding diagrams for other observational points are similar in form. Since the combination $\nu(1+z)$ enters into the spectrum, the curves corresponding to an observation with higher ν will vary more rapidly with z while the curves from infrared observations will be almost flat. In Figs 6 and 7 we give the strongest limit at any wavelength for each redshift, effectively superimposing diagrams like Fig. 5 for the various observational points and taking their lower envelope as the overall constraint.

The first results we present are those for a dust-free universe. The combined limits on Ω_* as a function of redshift are plotted in Fig. 6 for the three spectral models. The limits presented in Fig. 6 are significantly weaker than the approximate limits plotted in Fig. 4 of Carr *et al.* (1984). The redshift dependence of the R model limits is complicated because the different redshift ranges corresponding to the Lyman line are redshifted into different observational bands. The limits are quite good for the redshift ranges where this occurs, but where the are gaps in the observational coverage the limits are from the continuum and are much poorer. In a more realistic model the finite extent in redshift of the Population III era should smooth out most of these gaps.

To summarize the data we define a redshift $z(\Omega_*)$ below which a model is excluded; the star density can only be as much as Ω_* if the stars form at a redshift greater than $z(\Omega_*)$. We tabulate

© Royal Astronomical Society • Provided by the NASA Astrophysics Data System

1986MNRAS.223..763M

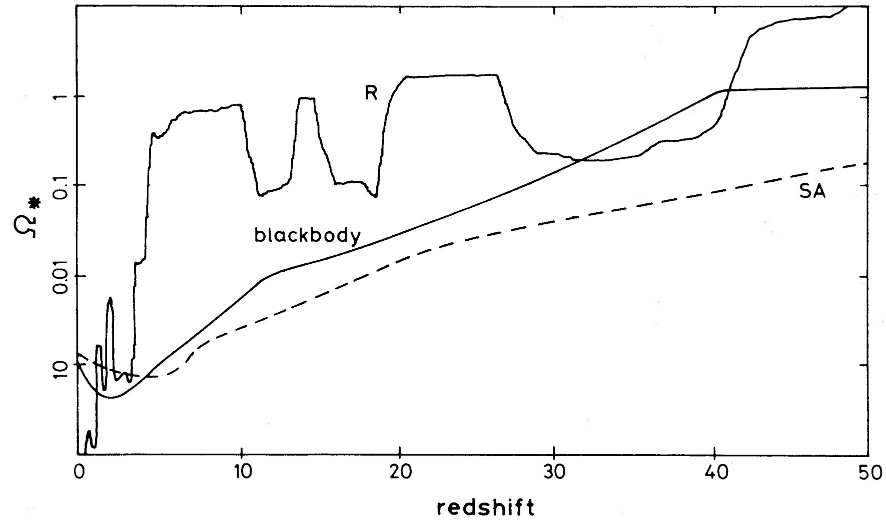

Figure 6. Limits for a dust-free universe. This diagram shows the maximum Ω_* that does not produce a background exceeding any of the observational limits of Table 1. The three curves represent the blackbody model, the hydrogen stellar atmosphere model (SA) and the recombination model (R).

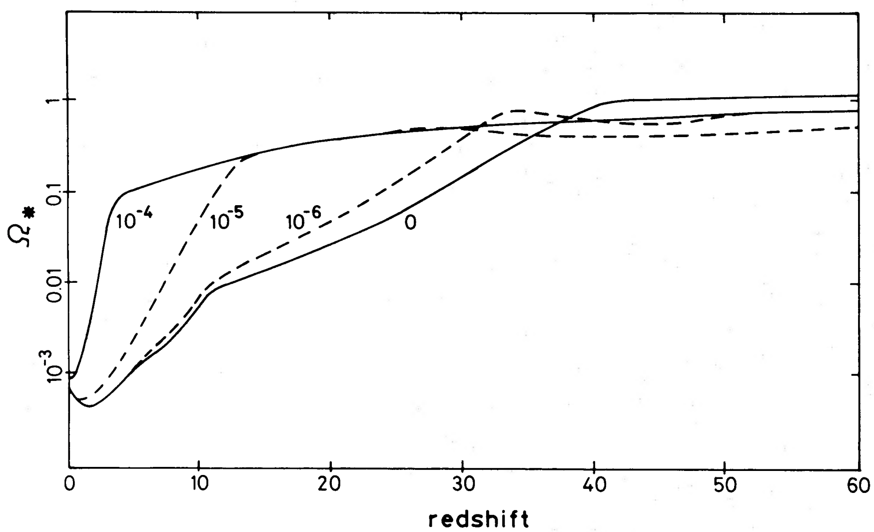

Figure 7. Limits for a dusty universe. This diagram shows the change in the blackbody model limit of Fig. 6 caused by taking into account various amounts of intergalactic dust. The curves are labelled with the corresponding value of the dust cosmological density parameter Ω_d.

$z(\Omega_*)$ for Ω_* values of 0.01, 0.1 (the minimum density usually postulated for the dark matter) and 1 (closure density). If z were as large as the redshift at which the age of the Universe equals the main-sequence time, then that model could be completely ruled out. In practice this is not the case with current observational limits, but very modest improvements in the observations would rule out many of the no-dust models (Table 2a).

Fig. 7 and Table 2(b) show the results obtained for the blackbody spectral model for varying dust abundances, under the assumption that the dust and the stars formed at the same epoch. As the dust abundance increases, the limit on dark-matter Population III stars becomes much weaker as it depends only on the weak far-infrared limits. The limit on a closure density of stars does not show this behaviour and is actually stronger that in the dust-free case. This is because the spectra of the high-redshift dust-emission models become narrower in frequency range as the

© Royal Astronomical Society • Provided by the NASA Astrophysics Data System

1986MNRAS.223..763M

redshift increases, leaving the peak energy relatively constant even though the total energy decreases. The limit does not therefore weaken with redshift in the usual way. The limits for the unabsorbed model are particularly weak as the peak of the redshifted blackbody spectrum lies in an unobserved region of the near infrared.

The models with dust at low redshift ($z=3, 5$) and maximum dust abundance (Table 2c) give only a slightly stronger constraint for $z(0.1)$. The constraint in these models at high redshift is the 200 μm limit on the intensity of the re-radiated emission from dust. It should be noted that the Woody & Richards and the *IRAS* points give a constraint which is weaker by a factor of 5, so that the 200 μm point is important and more observations in this region would be very useful.

8 Conclusion

Conditions in the earlier stages of the Universe's history may have led to the formation of stars of types whch no longer exist today. If large numbers of very massive stars were formed, they would leave remnants which could provide the dark matter. The radiation emitted by such objects would not be highy redshifted but would be present in amounts comparable with existing limits on the background light. If the radiation has not been scattered by dust, the constraints provided by this background light suggest that most of the mass in the Universe could not have been in such stars during the redshift range of a few to 20, commonly associated with galaxy formation and the immediate pregalactic era. Even if the intergalactic medium contains the maximum amount of dust consistent with observation, massive stars at a redshift of less than 4 cannot provide the dark matter. Observations by the *COBE* satellite (Mather 1982) later this decade should improve the observational constraints substantially. If there was significant pregalactic astrophysical activity, it should have produced a detectable infrared or ultraviolet radiation background.

Acknowledgments

I thank my supervisor Bernard Carr for suggesting the problem and for advice and helpful criticisms throughout the work, and Martin Rees, Dick Bond, Janet Drew and John Negroponte for helpful discussions. I acknowledge a Science and Engineering Research Council studentship and a studentship from the Cambridge Philosophical Society. I gratefully acknowledge the useful comments made by M. Rowan-Robinson on an earlier version of this paper.

References

Abramowicz, M. & Stegun, I. A., 1965. *Handbook of Mathematical Functions,* Dover, New York.
Baker, J. G., Menzel, D. H. & Aller, L. H., 1938. *Astrophys. J.,* **88,** 422.
Blitz, L., Fich, M. & Kulkarni, S., 1983. *Science,* **220,** 1233.
Bond, J. R., Arnett, W. D. & Carr, B. J., 1984. *Astrophys. J.,* **280,** 825.
Bond, J. R., Carr, B. J. & Hogan, C., 1986. Preprint.
Carr, B. J., 1979. *Mon. Not. R. astr. Soc.,* **189,** 123.
Carr, B. J., Bond, J. R. & Arnett, W. D., 1984. *Astrophys. J.,* **277,** 445.
Carr, B. J., McDowell, J. C. & Sato, H., 1983. *Nature,* **306,** 666.
Ceccarelli, C. *et al.*, 1984. *Astrophys. J.,* **275,** L39.
Couchman, H. M. P., 1985. *Mon. Not. R. astr. Soc.,* **214,** 137.
De Bernardis, P., Masi, S., Melchiorri, F. & Moreno, G., 1984. *Astrophys. J.,* **278,** 150.
Draine, B. T. & Lee, H. M., 1984. *Astrophys. J.,* **285,** 89.
Dube, R. R., Wicks, W. C. & Wilkinson, D. T., 1979. *Astrophys. J.,* **232,** 333.
Feldman, P. D., Brune, W. H. & Henry, R. C., 1981. *Astrophys. J.,* **249,** L51.
Hauser, M. *et al.* 1984. *Astrophys. J.,* **278,** L15.
Henry, R. C., Feldman, P. D., Fastie, W. G. & Weinstein, A., 1978. *Astrophys. J.,* **223,** 437.
Hoffman, W. & Lemke, D., 1978. *Astr. Astrophys.,* **68,** 389.

© Royal Astronomical Society • Provided by the NASA Astrophysics Data System

1986MNRAS.223..763M

Howarth, I., 1983. *Mon. Not. R. astr. Soc.,* **203,** 301.
Hoyle, F., Solomon, P. M. & Wolf, N. J., 1973. *Astrophys. J.,* **185,** L89.
Kaplan, S. A. & Pikel'ner, S. B., 1970. *The Interstellar Medium,* Harvard University Press, Cambridge, MA.
Layzer, D. & Hively, R. M., 1973. *Astrophys. J.,* **179,** 361.
Mather, J. C., 1982. *Opt. Eng.,* **21** (4), 769.
Matsumoto, T., Akiba, M. & Murakami, H., 1984. *Adv. Space Res.,* **3,** 469.
Maucherat-Joubart, M., Deharveng, J. M. & Cruvellier, P., 1980. *Astr. Astrophys.,* **88,** 323.
McDowell, J. C., 1985. *Mon. Not. R. astr. Soc.,* **217,** 77.
Negroponte, J., 1986. *Mon. Not. R. astr. Soc.,* **222,** 19.
Negroponte, J., Rowan-Robinson, M. & Silk, J., 1981. *Astrophys. J.,* **248,** 58.
Ostriker, J. & Heisler, J. M., 1984. *Astrophys. J.,* **278,** 1.
Peebles, P. J. & Partridge, R. B., 1967. *Astrophys. J.,* **148,** 377.
Rees, M. J., 1978. *Nature,* **275,** 35.
Rowan-Robinson, M., 1986. *Mon. Not. R. astr. Soc.,* **219,** 737.
Savage, B. D. & Mathis, J. S., 1979. *Ann. Rev. Astr. Astrophys.,* **17,** 73.
Severniyl, A. & Zverezda, A., 1983. *Astrophys. Lett.,* **23,** 71.
Spitzer, L. Jr, 1978. *Physical Processes in the Interstellar Medium,* Wiley, London.
Thorstensen, J. R. & Partridge, R. B., 1975. *Astrophys. J.,* **200,** 527.
Toller, G., 1983. *Astrophys. J.,* **266,** L79.
Weller, C. S., 1983. *Astrophys. J.,* **268,** 899.
Wesemael, F., Auer, L. H., Van Horn, H. M. & Savedoff, M. P., 1980. *Astrophys. J. Suppl.,* **43,** 159.
White, S. D. M. & Rees, M. J., 1978. *Mon. Not. R. astr. Soc.,* **183,** 341.
Woody, D. P. & Richards, P. L., 1981. *Astrophys. J.,* **248,** 18.
Wright, E. L., 1981. *Astrophys. J.,* **250,** 1.

© Royal Astronomical Society • Provided by the NASA Astrophysics Data System